

## Energy-resolved He-atom-scattering study of Ag(110) up to 900 K

G. Bracco, L. Pedemonte, and R. Tatarek

*Unità Istituto Nazionale Fisica della Materia and CFSBT/Consiglio Nazionale delle Ricerche,  
Via Dodecaneso 33, I-16146 Genova, Italy*

(Received 19 January 1996; revised manuscript received 28 May 1996)

A detailed study of the specular peak shape evolution with the Ag(110) surface temperature is presented. Time-of-flight measurements were performed along  $\langle 1\bar{1}0 \rangle$  and in the out-of-phase scattering condition to complete a previous work carried out in the  $\langle 001 \rangle$  direction. In particular, the effect of inelasticity on the roughening temperature evaluation is critically discussed. [S0163-1829(96)04439-6]

The thermal behavior of the (110) surface of various fcc metals was widely studied both theoretically<sup>1,2</sup> and experimentally with different techniques as x-ray,<sup>3</sup> He-atom,<sup>4</sup> and electron diffraction.<sup>5,6</sup> Among these surfaces, silver holds a central position since in the last years contradictory results were found about it. In fact, the classical roughening theory (CRT) developed from the pioneering work of Burton, Cabrera, and Frank<sup>7</sup> predicts that, at a critical temperature  $T_r$ , a low index surface undergoes an order-disorder transition because of the proliferation of thermally induced steps. Roughening causes the height difference correlation function  $C(\vec{R}) = \langle [h(\vec{0}) - h(\vec{R})]^2 \rangle$  to diverge logarithmically with increasing  $|\vec{R}|$  along the surface. Consequently, the elastically diffracted intensity  $I$  assumes, for a small momentum transfer  $Q$  parallel to the surface, a characteristic power-law behavior  $I \propto Q^{-(2-\tau)}$ . The exponent  $\tau$  gives a direct estimation of the surface roughness attaining a value 1 at  $T_r$  and in out-of-phase scattering conditions.<sup>1</sup> These results were confirmed for Ag(110) by Held *et al.*,<sup>3</sup> who estimated  $T_r = 725 \pm 25$  K, and by Bracco *et al.*,<sup>8</sup> who measured  $T_r = 910 \pm 15$  K, though restricting their study to the  $\langle 001 \rangle$  crystal direction. On the other hand, Robinson *et al.*<sup>9</sup> suggested a roughening of Ag(110) caused by the redistribution among flat and rough phases already coexisting on the surface at temperatures well below the critical one. In that hypothesis,  $T_r$  depends on the miscut angle  $\alpha$ . The authors introduced this model to explain the data obtained in the  $\langle 1\bar{1}0 \rangle$  azimuth along which the miscut of the sample was mainly directed. They measured  $T_r = 790$  K, with  $\alpha = 0.14^\circ$  and extrapolated  $T_{r,0} = 992$  K for the  $\alpha = 0^\circ$  surface. The model succeeded in justifying the estimation of Held *et al.*,<sup>3</sup> while a comparison with the results of Bracco *et al.*<sup>8</sup> seemed futile because of the different crystal directions involved in the experiments. Another question arose about the possibility to verify the prediction of the CRT. In fact, it was recently shown that the evolution toward a power-law shape of the diffracted peaks on increasing the sample temperature can be obscured by a crossover of the short-range behavior of the height-height correlation function to the asymptotic one at distances comparable to the instrumental transfer width.<sup>10</sup> In this case, to point out the prevailing short-range behavior of  $C(\vec{R})$ , the inelastic contribution to the scattered intensity has to be carefully rejected. This also avoids alterations of the

peak shape due to single-phonon and multiphonon events which reduce the estimated value of  $T_r$ .<sup>11</sup>

To contribute to the above arguments, we carried out an energy-resolved He-atom scattering study of Ag(110) in the 420–900-K temperature range with measurements performed along  $\langle 1\bar{1}0 \rangle$ . Thereafter, the collected time-of-flight (TOF) spectra were carefully analyzed to extract their elastic content. At first this allowed us to check on the crossover of the height-height correlation function up to distances of about 350 Å. Once we excluded that hypothesis, we performed a detailed study of the Ag(110) thermal behavior, pointing out the effect of single-phonon and multiphonon contributions to the scattered intensity on the critical temperature estimation.

To obtain the present results, the scattering apparatus described in Ref. 12 was improved, reducing the effective angular resolution of the detector to  $0.2^\circ$ . Moreover, a rotatable source was used to change the total deflection angle  $\theta_t$  between the incident beam and the detector axis in the range  $88/130^\circ$ . Because of the experimental conditions (incident wave vector  $k_i = 5.78 \text{ \AA}^{-1}$ , and beam energy  $E_b = 17.5$  meV), we achieved the best sensitivity to surface disorder by setting  $\theta_t = 112.25^\circ$ , thus matching the antiphase scattering condition for the specular peak better than 1% in the range between room temperature and the silver melting point.

The Ag sample was spark cut from a single crystal and chemomechanically polished. Its miscut, revealed with Laue diffraction, was  $\sim 0.15^\circ$ , mainly directed along  $\langle 1\bar{1}0 \rangle$ , thus similar to that of Robinson *et al.*<sup>9</sup> The sample was heated radiatively, and its temperature  $T_s$  measured with a  $K$ -type thermocouple welded on the crystal edge. The overall uncertainty on  $T_s$  was  $\sim 15$  K.

To prevent the segregation of bulk impurity atoms which were also shown to facet the surface at very low coverages,<sup>13,14</sup> different sample preparations were tried.<sup>15</sup> An example of the specular line-shape dependence on the cleaning procedure is shown in Fig. 1. The full width at half maximum (FWHM) of the broad peak is  $\gamma = 0.41^\circ$ . It was measured at  $T_s = 600$  K after room-temperature  $\text{Ar}^+$ -ion sputtering and annealing at  $T_s = 700$  K for 10 min. Several structures are recognizable inside the specular profile. They suggested a surface morphology similar to that described in Ref. 9. Since freshly sputtered surfaces did not show similar features which were easily recovered annealing the sample at

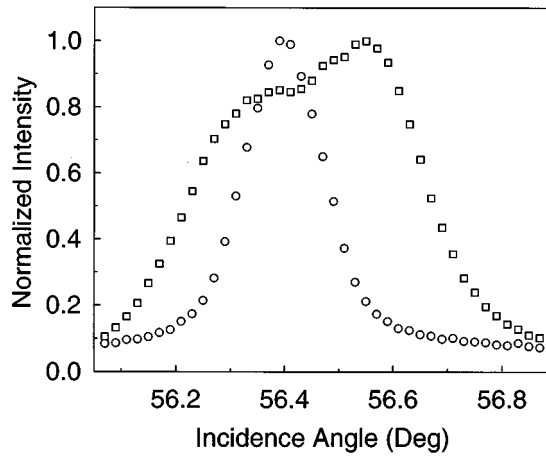


FIG. 1. Specular peak profiles measured on Ag(110) along  $\langle 1\bar{1}0 \rangle$  at surface temperature  $T_s=600$  K after different cleaning procedures: (□) Room-temperature ion sputtering at 1 keV and annealing at  $T_s=700$  K for 10 min. (○) Same procedure as before followed by several days of low energy (120 eV) ion sputtering at  $T_s=600$  K. Helium beam energy  $E_b=17.5$  meV, total angle  $\theta_t=112.8^\circ$ .

$T_s \geq 550$  K, we cleaned the surface for several days with low-energy ( $< 300$  eV) ion sputtering at  $T_s=600$  K. No structures are now detectable in the specular line shape shown in Fig. 1, whose FWHM is  $0.17^\circ$ , close to the value  $0.15^\circ$  obtained from computer simulations of the scattering apparatus. Moreover, the peak shape was stable for more than 22 h, the maximum time we checked it. These results suggested that we clean the sample before each set of measurements performed at fixed temperature by prolonged ( $> 15$  h) low-energy sputtering which most probably removed the light contaminants of silver, i.e., C and/or S.<sup>13,14</sup> In spite of the careful preparation, the peak shape degraded in a few hours above 900 K, thus preventing the extension of our study to higher temperatures. To avoid defect freezing and nonequilibrium states of the surface, low cooling and heating rates (10 K/min) were used.

To obtain the specular peak profiles between 420 and 900 K, 33 TOF spectra were collected at each sample temperature in the range  $\pm 0.8^\circ$  around the (0,0) direction, and analyzed in detail to extract the elastic contribution to the scattering. This was accomplished fitting each TOF spectrum by the sum of three functions plus a constant. An example is shown in Fig. 2. The thin solid and dotted lines represent the elastic and single-phonon scattering peak, respectively. They were described by the convolution of the translated Maxwellian velocity distribution of the incoming He beam,<sup>16</sup> with the Dirac  $\delta$  expressing the energy conservation law. In the small phonon energy exchange limit, both peaks could be fitted with a function of the form  $f(t) = A(t_0/t)^5 \exp\{-[(t_0/t)-1]^2/\sigma^2\}$ , with  $A$ ,  $t_0$ , and  $\sigma$  the fitting parameters. The dashed line represents the multiphonon scattering described in the extreme semiclassical limit, and for light point particles diffracting from a heavy atoms lattice, as reported in Ref. 17. The constant, not shown in the figure, takes into account the He background in the detector stage. Thereafter, the integrated intensity of each elastic

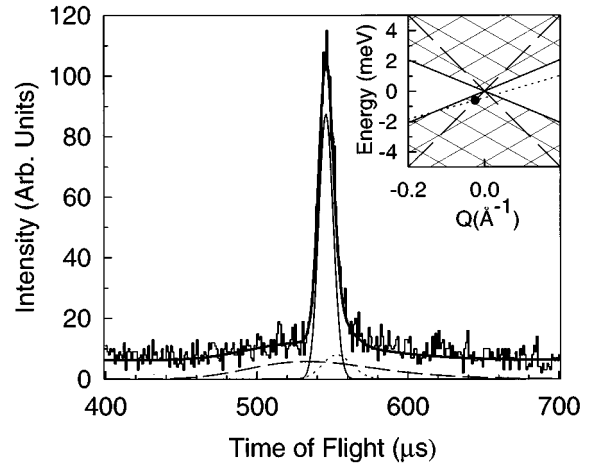


FIG. 2. An example of the analysis performed on the time-of-flight spectra. The thin solid, dotted, and dashed lines are the best-fit curves which represent the elastic feature, the single-phonon peak, and the multiphonon background, respectively. The sum of these contributions plus a constant is shown by the thick solid line. The inset shows part of the Ag(110) phonon spectrum along  $\langle 1\bar{1}0 \rangle$  in the  $(\hbar\omega, Q)$  plane. The surface-projected bulk phonon modes, the Rayleigh wave  $S_1$ , and the threshold of the bulk longitudinal vibrations are represented by shaded regions, solid lines, and dashed lines, respectively. The dotted line is the kinematical scan curve of the reported spectrum, and the full circle corresponds to the inelastic peak position.  $T_s=750$  K,  $\theta_t=112.25^\circ$ , and incident angle  $\theta_i=56.90^\circ$ .

structure having a FWHM  $\sim 0.4$  meV was used to construct the angular profile at a given temperature. Finally it was converted into a parallel momentum-transfer scale  $Q$  through the relations  $Q = 2k_i \cos\theta_i \sin\theta_t$ ,  $I(Q) = JI(\theta_i)$ , where  $\theta_i$  is the incidence angle,  $I$  the peak intensity, and  $J$  the Jacobian of the transformation.

At first, to exclude prevailing crossover effects of the height difference correlation function,<sup>10</sup> the peak profiles measured at several  $T_s$  were plotted versus the momentum transfer  $Q$ , each scaled with its own FWHM, as shown in the inset of Fig. 3. If the onset length of the asymptotical behavior of  $C(\vec{R})$  is comparable to the instrumental transfer width, the line shapes should fall upon each other. Their evolution with the sample temperature pointed out that a study of the long-range behavior of  $C(\vec{R})$ , and hence of the roughening, was accessible.

This result stimulated us to follow the thermal disordering of Ag(110) through the evolution of the diffracted line shape, as shown in Fig. 3. Since at  $T_s \ll T_r$  the specular profile consists of a sharp peak (the Bragg peak) and diffuse low intensity tails arising from local steps, the profile measured at  $T_s=420$  K was fitted as a superposition of Gaussian and Lorentzian functions. The FWHM of the Gaussian representing the instrument response function was  $0.018 \text{ \AA}^{-1}$ , to which corresponds a transfer width of about 350 Å. As the surface temperature increases, the specular peak broadens, and the peak-to-tail intensity ratio decreases, until at  $T_s=900$  K the Gaussian shape is lost. To describe the peak evolution the data above  $T_s=600$  K were fitted with a power-law function predicted by the CRT. To avoid decon-

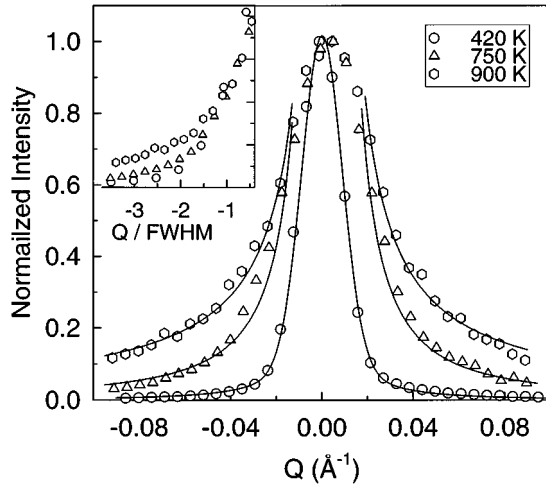


FIG. 3. Specular peak profiles measured along  $\langle 1\bar{1}0 \rangle$  at different surface temperatures.  $Q$  is the momentum transfer parallel to the surface. The solid lines are the best-fitting curves described in the text. The inset shows the left tail of the same distributions each scaled with its own full width at half maximum. This value changes between  $0.023 \text{ \AA}^{-1}$  at  $T_s = 420 \text{ K}$  and  $0.054 \text{ \AA}^{-1}$  at  $T_s = 900 \text{ K}$ .

volution with the instrument response function, the momentum-transfer range outside the FWHM of the peak profile measured at  $T_s = 420 \text{ K}$  was considered. The obtained  $\chi^2$  value reduces from more than 10 at  $T_s \sim 600 \text{ K}$  to 1.5 at  $900 \text{ K}$ .

The surface disordering suggested by the peak broadening was quantified reporting the roughness index  $\tau$  versus the surface temperature; see Fig. 4. Open circles were obtained from the TOF spectra analysis previously described, thus considering the elastic contribution only. We can observe that  $\tau$  remains approximately constant and small up to about  $600 \text{ K}$ ; then it grows progressively. The opposite behavior is shown above  $600 \text{ K}$  by the logarithmic integrated peak intensity reported with filled circles in the same figure, once the familiar Debye-Waller behavior was factored out. This allowed us to fix the onset of the Ag(110) roughening at  $T_s = 600 \text{ K}$ . Since  $\tau$  is slightly lower than 1 even at  $T_s = 900 \text{ K}$ , we may suppose the Ag(110) surface to roughen at  $T_r > 900 \text{ K}$ . In order to point out the effect of inelasticity on this estimation, the  $\tau$  values obtained with a reduced energy filtering of the TOF spectra were also reported in Fig. 4. To do this, peak profiles were constructed extracting from every spectrum the intensity collected in an energy window  $\Delta E$  centered at the elastic time. Open squares and open diamonds correspond to  $\Delta E = 0.7$  and  $7 \text{ meV}$ , thus attaining the critical value  $\tau = 1$  at  $T_r \sim 850$  and  $800 \text{ K}$ , respectively. Thus the  $\tau$  behavior seemed to be strongly dependent on the energy resolution.<sup>11,18,19</sup>

The data reported here show a good agreement with most of the results reported in the literature. As regard as our work along the  $\langle 001 \rangle$  azimuth,<sup>8</sup> the reduction by about  $100 \text{ K}$  observed at the onset of roughening can be understood in light of the described improvements of the scattering apparatus, which now allows a higher sensibility to surface defects. The present estimation of the roughening temperature compares

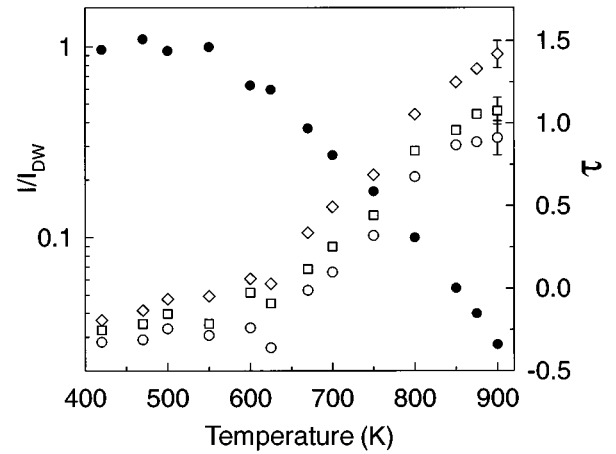


FIG. 4. Open symbols show the best-fit value of the roughness index  $\tau$  vs the surface temperature obtained with different analysis of the time-of-flight spectra: (○) Elastic scattering only. (□) Energy window  $\Delta E = 0.7 \text{ meV}$ . (◇)  $\Delta E = 7 \text{ meV}$  (for more details see text). The error bars account for both the effect of repeated measurements and the uncertainty of the fitting parameters. Solid circles show the integrated specular peak intensity  $I$  normalized by a linear Debye-Waller factor  $I_{\text{DW}}$  plotted vs the surface temperature. Now the symbol dimension is representative of the error bar.

favorably both with the value  $T_r = 910 \pm 15 \text{ K}$  we fixed a few years ago, and the molecular-dynamics calculations performed by Rahman and Tian,<sup>20</sup> setting  $T_r = 930 \text{ K}$ . Also the roughening temperature estimated by Robinson *et al.* for the ideal surface,  $T_{r,0} = 992 \text{ K}$ , appears reasonable if the approximations they made to determine it were taken into account.<sup>9</sup>

To explain the lower  $T_r$  value measured by Held *et al.*,<sup>3</sup> we note that even an impurity coverage well below the resolution of the Auger spectroscopy can decrease the surface roughening temperature because of the defect energy cost reduction, which encourages step proliferation. Indeed, specular line shapes measured at  $T_s \sim 800 \text{ K}$  after an improper cleaning treatment showed an already rough sample.

Finally, we observe that, although we rejected all inelastic contributions in the TOF spectra, no crossover of the height correlation function toward logarithmic behavior was detected over distances comparable with the transfer width of the scattering apparatus. This contrasts with the results of Ernst, Folkerts, and Schwenger,<sup>10</sup> who observed such crossover on a stepped Cu(115) surface, but it agrees with Monte Carlo simulations<sup>21</sup> and with x-ray scattering experiments.<sup>22</sup>

In conclusion, our energy-resolved He-atom measurements on Ag(110) allowed us to furnish a detailed description of surface disordering which confirmed the CRT prediction of Ag(110) roughening driven by thermally induced step proliferation. We pointed out that the inelastic contribution to the scattered intensity or an improper sample cleaning might cause an underestimation of the critical temperature. Thus measurements on *real* samples, although carefully performed, can provide only a lower limit.

We gratefully acknowledge partial support to the project ‘‘Hot Surfaces’’ from the Italian National Research Council.

- <sup>1</sup>A. Trayanov, A.C. Levi and E. Tosatti, *Surf. Sci.* **233**, 184 (1990).
- <sup>2</sup>C. Jayaprakash and W.F. Saam, *Phys. Rev. B* **30**, 3916 (1984).
- <sup>3</sup>G.A. Held, J.L. Jordan-Sweet, P.M. Horn, A. Mak, and R.J. Birgenau, *Phys. Rev. Lett.* **59**, 2075 (1987); *J. Phys. (Paris) Colloq.* **50**, C7-245 (1989).
- <sup>4</sup>J. Sproesser, B. Salanon, and J. Lapujoulade, *Europhys. Lett.* **16**, 283 (1991).
- <sup>5</sup>Y. Cao and E.H. Conrad, *Phys. Rev. Lett.* **64**, 447 (1990).
- <sup>6</sup>H.N. Yang, T.M. Lu, and G.C. Wang, *Phys. Rev. Lett.* **15**, 1621 (1989).
- <sup>7</sup>W.K. Burton, N. Cabrera, and F.C. Frank, *Philos. Trans. R. Soc. London Ser. A* **243**, 299 (1951).
- <sup>8</sup>G. Bracco, C. Maló, C.J. Moses, and R. Tatarek, *Surf. Sci.* **287/288**, 871 (1993).
- <sup>9</sup>I.K. Robinson, E. Vlieg, H. Hoernis, and E.H. Conrad, *Phys. Rev. Lett.* **67**, 1890 (1991); *Surface X-Ray and Neutron Scattering*, edited by H. Zabel and I.K. Robinson, Springer Proceedings in Physics Vol. 61 (Springer-Verlag, Heidelberg, 1992), p. 73.
- <sup>10</sup>H.J. Ernst, R. Folkerts, and L. Schwenger, *Phys. Rev. B* **52**, 8461 (1995).
- <sup>11</sup>G. Bracco, C. Maló, L. Pedemonte, and R. Tatarek, *J. Electron. Spectrosc. Relat. Phenom.* **64/65**, 10 155 (1993).
- <sup>12</sup>G. Bracco, R. Tatarek, S. Terreni, F. Tommasini, and U. Linke, *J. Electron. Spectrosc. Relat. Phenom.* **44**, 197 (1987).
- <sup>13</sup>J.S. Ozcomert, W.W. Pai, N.C. Bartelt, and J.E. Reutt-Robey, *Surf. Sci.* **293**, 183 (1993).
- <sup>14</sup>G.A. Held, D.M. Goodstein, R.M. Feenstra, M.J. Ramstad, D.Y. Noh, and R.J. Birgenau, *Phys. Rev. B* **48**, 1933 (1993).
- <sup>15</sup>G. Bracco, L. Pedemonte, and R. Tatarek, *Surf. Sci.* **353/354**, 968 (1996).
- <sup>16</sup>D.R. Miller, *Free Jet Sources, Atomics and Molecular Beam Methods*, edited by G. Scoles (Oxford University Press, New York, 1988), Vol. 1, p. 14.
- <sup>17</sup>J.R. Manson, *J. Electron. Spectrosc. Relat. Phenom.* **64/65**, 151 (1993).
- <sup>18</sup>M. den Nijls, E.K. Riedel, E.H. Conrad, and T. Engel, *Phys. Rev. Lett.* **55**, 1689 (1985).
- <sup>19</sup>M. den Nijls, E.K. Riedel, E.H. Conrad, and T. Engel, *Phys. Rev. Lett.* **57**, 1279 (1986).
- <sup>20</sup>T.S. Rahman and Z.J. Tian, *J. Electron. Spectrosc. Relat. Phenom.* **64/65**, 651 (1993); and (private communication).
- <sup>21</sup>N.C. Bartelt, T.L. Einstein, and E.D. Williams, *Surf. Sci.* **276**, 308 (1992).
- <sup>22</sup>D.L. Abernathy, S.G.J. Mochrie, D.M. Zehner, G. Gruebel, and D. Gibbs, *Phys. Rev. Lett.* **69**, 941 (1992).